Chromium-Alloyed PM Steels with Excellent Fatigue Properties Obtained by Different Process Routes

Ola Bergman

Höganäs AB, Sweden

ABSTRACT

Chromium is an attractive alloying element in steels due to its positive effect on the hardenability, its low cost and environmental benefits. These advantages are utilised in two recently developed pre-alloyed water-atomised PM grades. Astaloy CrL, which contains 1.5% Cr and 0.2% Mo, and Astaloy CrM, which contains 3% Cr and 0.5% Mo, are suitable for high-performance applications. This paper is focused on the fatigue properties of these materials. The bending fatigue limits at sintered density 7.1 g/cm^3 are 261 MPa for Astaloy CrL + 0.8% graphite and 287 MPa for Astaloy CrM + 0.45% graphite after conventional sintering at 1120 ºC. High temperature sintering followed by rapid cooling increase the fatigue limits of the materials by 20-30% to 320MPa and 372 MPa respectively. Moreover, Astaloy CrM + 0.45% graphite obtains a very high fatigue limit of 527 MPa at sintered density 7.3 g/cm^3 after high temperature sintering and vacuum-carburising.

INTRODUCTION

PM steels are becoming more widely used in highly stressed applications, such as con rods and gears, where high fatigue performance is required. Secondary operations are generally necessary to reach the desired fatigue properties, which leads to high production costs. However, this study shows that there are possibilities to obtain good dynamic as well as static mechanical properties from a single-stage sintering process, by making a clever choice of material and process route.

Density and microstructure are the key parameters for fatigue performance of PM steels. The fatigue strength increases with the density of the PM component [1], [2]. Still, at a given density the fatigue performance can vary considerably depending on the microstructure. A pearlitic Fe-Cu-C steel has a bending fatigue limit of 220 MPa at sintered density 7.1 g/cm^3 [3], while martensitic PM steels have been reported to reach bending fatigue limits of 380 MPa at the same density [1]. Consequently, much can be gained by optimising the microstructure of PM steels. Alloying elements that give high hardenability, such as chromium, offer possibilities to obtain high performance microstructures at relatively moderate cooling rates.

The fatigue performance of two different chromium-alloyed powder grades, Astaloy CrL and Astaloy CrM, has been investigated. Sinterings were performed at 1120 ºC and 1250 ºC for 30 minutes in 90% N_2/10% H_2. Two different cooling rates were applied (0.5-1 ºC/s and 2-3 ºC/s). High temperature sintering followed by vacuum-carburising was also tested for one powder mix. Plane bending fatigue tests, tensile tests, hardness measurements and metallography were performed on the sintered materials.

EXPERIMENTAL PROCEDURE

Two fully pre-alloyed water-atomised steel powders, Astaloy CrL and Astaloy CrM, were studied in this investigation (see Table 1). Three different test mixes were prepared based on these powder grades. The compositions of the test mixes are outlined in Table 2. Type of graphite used was Kropfmühl UF4 (96-97% C). For the cold compaction mixes, A and B, amide wax was used as lubricant while the warm compaction mix, C, was a Densmix®.

Powder Grade	**Cr (wt%)**	**Mo (wt%)**	**C (wt%)**	**O (wt%)**	**Fe (wt%)**
Astaloy CrL	1.5	0.2	<0.01	0.15	Bal.
Astaloy CrM	3.0	0.5	<0.01	0.20	Bal.

Table 1. Chemical compositions of investigated powder grades.

Test Mix	**Base Powder**	**Graphite (wt%)**	**Lubricant (wt%)**
A	Astaloy CrL	0.8	0.8
B	Astaloy CrM	0.45	0.8
C	Astaloy CrM	0.45	0.6

Table 2. Compositions of test mixes.

Standard (ISO 3928) fatigue test bars modified with chamfered edges [4] were produced for all three test mixes. Standard (ISO 2740) tensile test bars were also produced for mixes A and B. The test bars of mix A were cold compacted to green density 7.0 g/cm^3 for high temperature sintering and 7.1 g/cm^3 for conventional sintering. Furthermore, the test bars of mix B were cold compacted to a green density of 7.05 g/cm^3, while the test bars of mix C were warm compacted to a green density of 7.15 g/cm^3. For warm compaction, both the powder and the tool were heated to 120 ºC.

Test bars of mixes A and B were subjected to two different sintering conditions (see Table 3). Conventional sintering at 1120 ºC followed by normal cooling at 0.5-1 ºC/s (Process 1) was applied as well as high temperature sintering at 1250 ºC followed by rapid cooling at 2-3 ºC/s (Process 2). The sinter-hardened specimens were tempered at 180 ºC for 60 minutes in air.

	Process 1	**Process 2**
Temperature	1120 ºC	1250 ºC
Time	30 min.	30 min.
Cooling rate	0.5-1 ºC/s	2-3 ºC/s
Atmosphere	90% N_2 + 10% H_2	90% N_2 + 10% H_2

Table 3. Sintering conditions for test mixes A and B.

The warm compacted test bars of mix C were high temperature sintered at 1300 ºC for 30 minutes in a laboratory vacuum furnace (Process 3). Subsequently, the samples were cooled to 1050 ºC and then carburised with acetylene gas for a total of 8 minutes at this temperature. Thereafter, cooling was performed in an N_2 atmosphere at 2 bars pressure. In the next step, the samples were moved to another vacuum furnace where they were heated at 950 ºC for 15 minutes and then cooled with N_2 at 7 bars pressure. Finally, the samples were tempered at 200 ºC for 60 minutes in air.

Fatigue tests were carried out in 4 point plane bending mode at a frequency of 28 Hz and with load ratio $R = \sigma_{min}/\sigma_{max} = -1$. The fatigue limit σ_A (50% estimated survival value) was determined by the staircase method with a run out limit of 2 million cycles. Standard tensile tests were performed and Vickers hardness was measured. Metallography was conducted in light-optical microscope (LOM).

RESULTS

Mechanical properties

Results from tensile tests and hardness measurements on the sintered specimens are presented in Table 4 together with combined carbon contents and sintered densities.

Material (Mix-Process)	**C (wt%)**	**SD (g/cm^3)**	**TS (MPa)**	**YS (MPa)**	**A (%)**	**HV10**
A-1	0.78	7.10	899	739	1.4	267
A-2	0.66	7.12	1087	860	0.6	380
B-1	0.39	7.08	1014	658	1.2	291
B-2	0.33	7.14	1309	925	1.5	377
C-3	0.30	7.29	NT	NT	NT	507

Table 4. Carbon contents, sintered densities (SD) and results from tensile tests and hardness measurements on sintered specimens (tensile tests were not performed on material C-3).

The combined carbon contents reveal that carbon loss during sintering was more pronounced during high temperature sintering than during conventional sintering. Analysed oxygen contents were around 0.1% after sintering at 1120 ºC and below 0.03% after sintering at the higher temperatures. The high density (7.3 g/cm^3) of material C-3 is a consequence of warm compaction combined with high temperature sintering. All other materials have sintered densities close to 7.1 g/cm^3.

The tensile strength (TS) of material A is about 20% higher (1087 MPa) after high temperature sintering and rapid cooling as compared to after conventional sintering (899 MPa). For material B, the effect of higher sintering temperature and faster cooling is a 30% increase in tensile strength (1309 MPa compared to 1014 MPa). Material A-2 has an elongation (A) of 0.6%, while the other materials have elongation values between 1% and 1.5%. The hardness values of the sinter-hardened materials (A-2 & B-2) are substantially higher than the hardness values of the conventionally sintered materials (A-1 & B-1). The vacuum-carburised material C-3 has the highest hardness (507 HV10).

Fatigue performance

Plane bending fatigue limits of the studied materials are presented in Table 5 and Figure 1. Material A gave a fatigue limit of 261 MPa after conventional sintering and 320 MPa after high temperature sintering and rapid cooling, which means an increase in fatigue strength by 23%. The fatigue performance of these materials (A-1 & A-2) is described by the diagram in Figure 2. The data for material A-1 shows a relatively steep S-N curve, while material A-2 has a flatter curve with knee-point at a low number of load cycles.

For material B, the fatigue limit is 28% higher after high temperature sintering and rapid cooling (372 MPa) as compared to after conventional sintering (287 MPa). Furthermore, the performance of material C after warm compaction, high temperature sintering and vacuum-carburising shows that a very high fatigue limit of 527 MPa can be reached for the same base material (Astaloy CrM + 0.45% graphite). The diagram in Figure 3 illustrates the fatigue performance of these three materials (B-1, B-2 & C-3). All materials have relatively flat S-N curves. The scatter of the data points that define the S-N curves is small for materials B-1 and C-3, but relatively large for material B-2. The reason for this is treated in the discussion section of the article.

Material (Mix-Process)	A-1	A-2	B-1	B-2	C-3
$\sigma_{A, 50\%}$ (MPa)	261	320	287	372	527

Table 5. Plane bending fatigue limits determined by the staircase method.

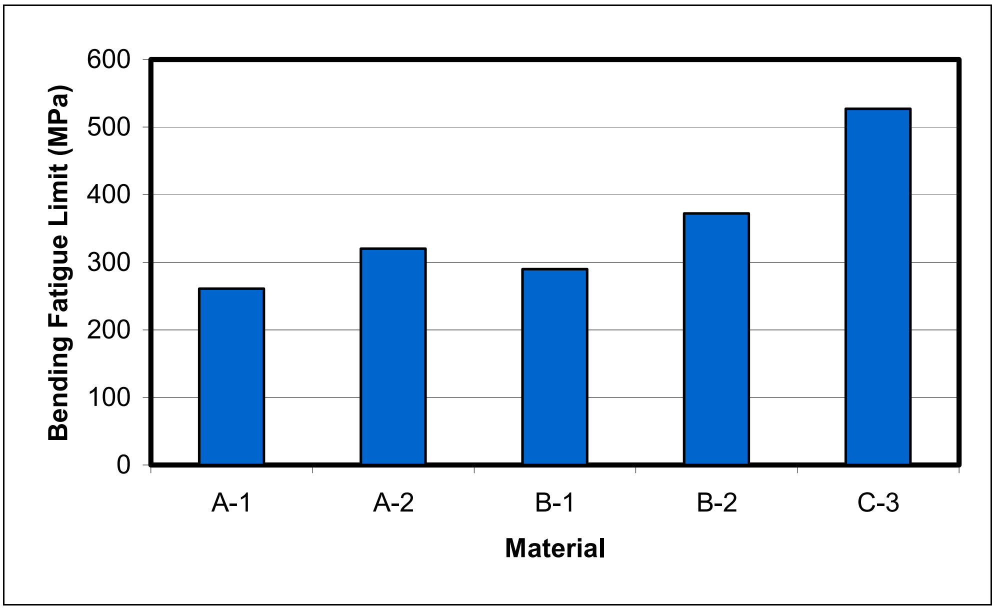

Figure 1. Plane bending fatigue limits of Cr-alloyed PM steels after different process routes.

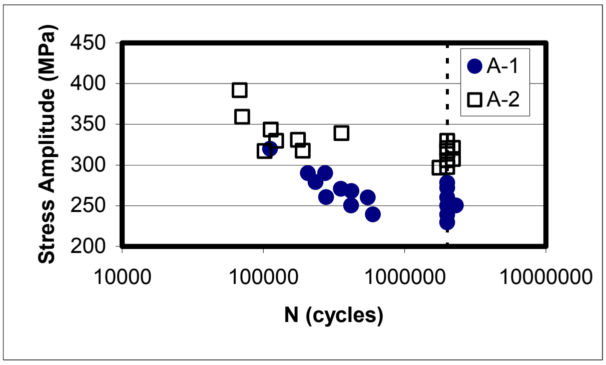

Figure 2. S-N diagram for materials A-1 & A-2 at fully reversed loading in plane bending.

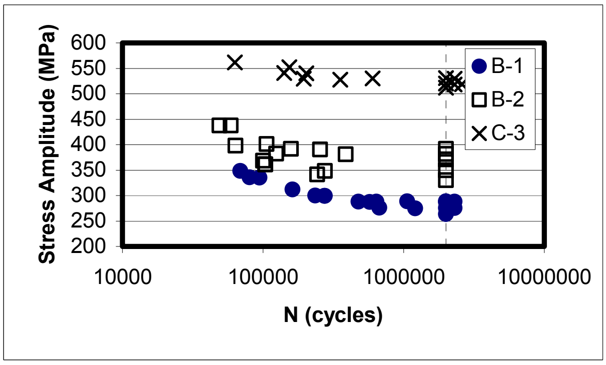

Figure 3. S-N diagram for materials B-1, B-2 & C-3 at fully reversed loading in plane bending.

Microstructures

The microstructure of material A-1 is dominated by lower bainite (see Figure 4). Some areas of upper bainite and martensite are also present in the structure. For material A-2, the microstructure consists of martensite mixed with 10-20% lower bainite.

Material B-1 has a relatively fine graded upper bainitic microstructure with some martensite present, whereas the microstructure of material B-2 contains a mixture of martensite (mainly) and lower bainite (see Figure 5). Consequently, for both material types (Astaloy CrL + 0.8% graphite & Astaloy CrM + 0.45% graphite) there is a shift in microstructure from bainite to mainly martensite as the cooling rate is increased from 0.5-1 ºC/s to 2-3 ºC/s. An effect of sintering temperature can also be observed, as the pores are rounder in the materials (A-2 & B-2) sintered at 1250 ºC than in the materials (A-1 & B-1) sintered at 1120 ºC.

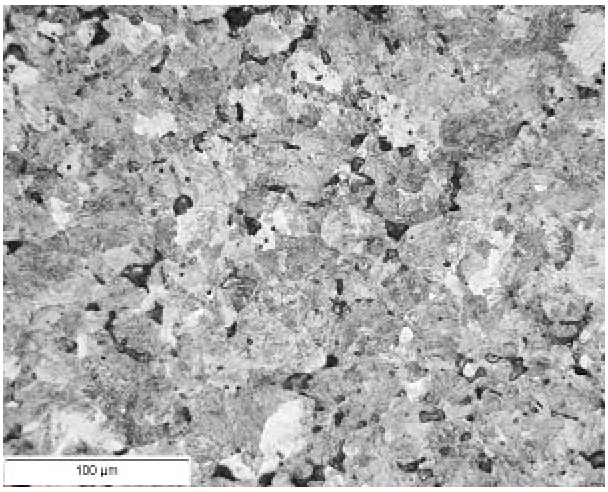

Figure 4. Microstructure of material A-1 (Astaloy CrL + 0.8% graphite, conventional sintering). Etched with Nital/Picral.

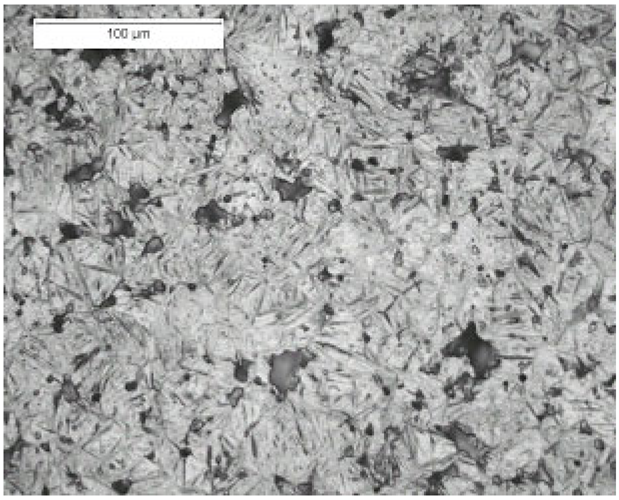

Figure 5. Microstructure of material B-2 (Astaloy CrM + 0.45% graphite, high temperature sintering and rapid cooling). Etched with Nital/Picral.

The microstructure of material C-3 shows a surface layer of martensite with some retained austenite and a few carbides. Apart from this surface layer, the microstructure is bainitic with some martensitic areas. Case hardening depth, defined as the distance from the surface at which the microhardness is below 550 HV0.1, was estimated to 0.4 mm.

DISCUSSION

This investigation shows that chromium-alloyed PM steel grades are suitable for applications where high fatigue performance is required. After conventional sintering at 1120 ºC, Astaloy CrL mixed with 0.8% graphite and Astaloy CrM mixed with 0.45% graphite obtain bending fatigue limits of 261 MPa and 287 MPa respectively. Furthermore, these fatigue limits increase by 20-30% at the same sintered density (7.1 g/cm^3) if the materials are high temperature sintered and sinter-hardened. Higher sintering temperature gives rounder pores, which is beneficial for the fatigue performance. However, the main reason for the gain in fatigue strength is the shift in microstructure that occurs as a higher cooling rate is applied.

The investigated materials have mainly bainitic microstructures after conventional sintering with a cooling rate of 0.5-1 ºC/s, whereas the microstructures are dominated by martensite after sinter-hardening at 2-3 ºC/s. This material behaviour is illustrated by the CCT (Continuous Cooling Transformation) diagram for Astaloy CrM + 0.4% C in Figure 6. At cooling rates between 0.5 ºC/s and 3 ºC/s, mixtures of bainite and martensite are obtained and the amount of martensite increases with the cooling rate. The fatigue strength of the material increases as the martensite content goes up, since martensitic microstructures are advantageous for the fatigue performance [1], [3].

Small variations in cooling rate in the interval 2-3 ºC/s leads to relatively large differences in the microstructure of Astaloy CrM + 0.4% C (see Figure 6). Thereby, the fatigue performance of the material may vary depending on if martensite or lower bainite is the dominating structure. This is why the scatter in fatigue data was rather large for sinter-hardened Astaloy CrM + 0.45% graphite in the performed investigation.

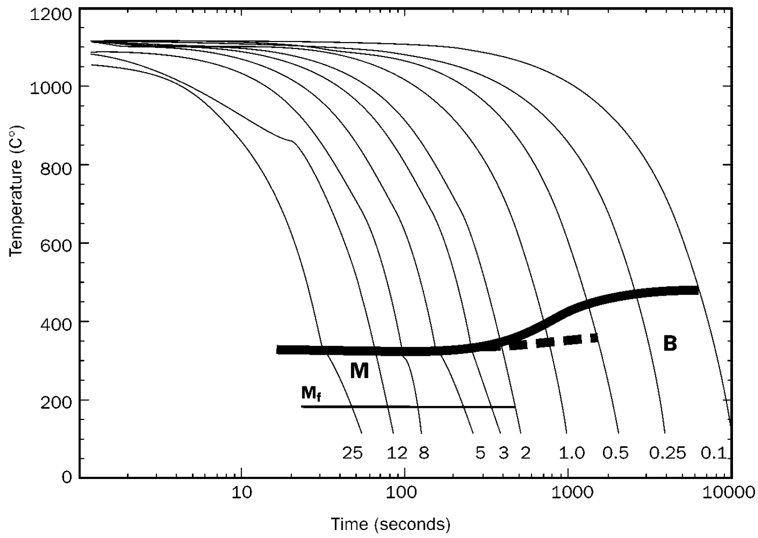

Figure 6. CCT diagram for Astaloy CrM + 0.4% C (B = Bainite, M = Martensite).

A similar effect gave certain scatter in fatigue data for Astaloy CrL + 0.8% graphite after cooling at 0.5-1 ºC/s. Microstructure variations regarding relative amounts of lower bainite and upper bainite lead to changes in fatigue performance. On the other hand, the material has a low scatter in fatigue data after rapid cooling at 2-3 ºC/s when martensite dominates the microstructure.

A very high bending fatigue limit of 527 MPa was obtained for high temperature sintered and vacuum-carburised Astaloy CrM + 0.45% graphite at sintered density 7.3 g/cm^3. Hence, a carburised martensitic surface layer leads to excellent fatigue performance of the material, although the rest of the microstructure is bainitic.

CONCLUSIONS

- The bending fatigue limits at sintered density 7.1 g/cm^3 are 261 MPa for Astaloy CrL + 0.8% graphite and 287 MPa for Astaloy CrM + 0.45% graphite after conventional sintering at 1120 ºC. High temperature sintering followed by rapid cooling increase the fatigue limits of the materials by 20-30% to 320MPa and 372 MPa respectively. The gain in fatigue performance is primarily due to a shift in microstructure from mainly bainitic to mainly martensitic.

- Astaloy CrM + 0.45% graphite obtains a very high fatigue limit of 527 MPa at sintered density 7.3 g/cm^3 after high temperature sintering and vacuum-carburising. The carburised martensitic surface layer strongly contributes to the excellent fatigue performance of the material.

REFERENCES

1. Sanderow, H.I., Spirko, J.R. and Friedhoff, T.G. "Fatigue properties of P/M materials: Relationship to RBF and AF results to Material-Processing Parameters", *Advances in Powder Metallurgy and Particulate Materials*, Vol. 2, pp. 117-135, 1997.
2. Bergmark, A. "Influence of density on PM steel fatigue crack initiation and propagation", *Advances in Powder Metallurgy and Particulate Materials*, Vol. 10, pp. 95-102, 2001.
3. Bergman, O. and Bergmark A. "Influence of microstructure on the fatigue performance of PM steels", *PM^{2}TEC 2003 Conference*, Las Vegas, June 8-12, 2003.
4. Bergmark, A., Alzati, L., Persson, U. "Fatigue crack initiation in PM Steels", *Advances in Powder Metallurgy and Particulate Materials*, Vol. 5, pp. 95-103, 2002.